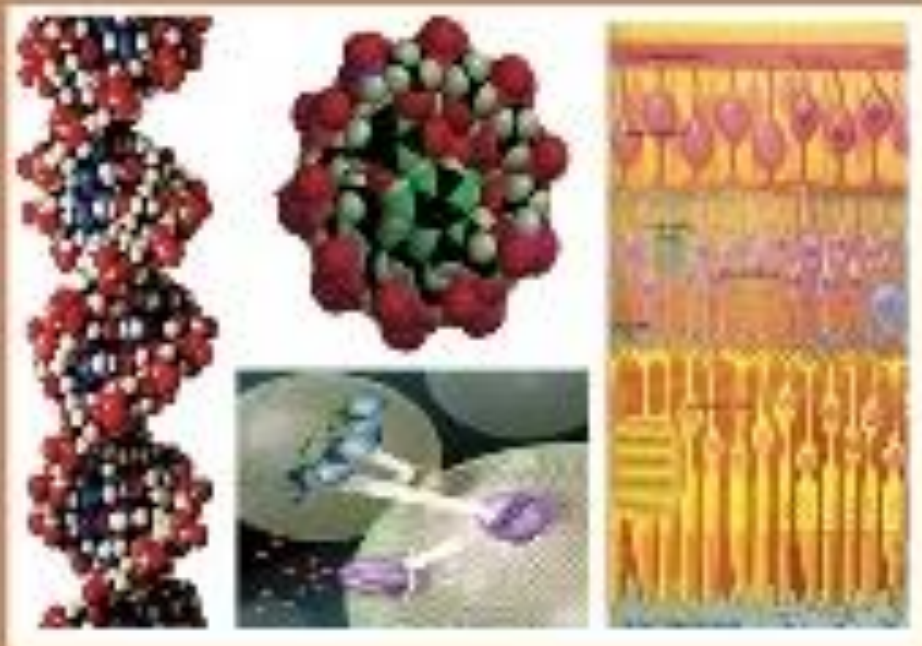




C

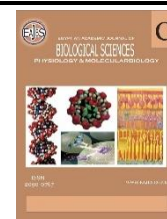
EGYPTIAN ACADEMIC JOURNAL OF  
**BIOLOGICAL SCIENCES**  
PHYSIOLOGY & MOLECULAR BIOLOGY



ISSN  
2090-0767

[WWW.EAJBS.ICA.NET](http://WWW.EAJBS.ICA.NET)

**Vol. 17 No. 2 (2025)**



## Shielding the Lungs: Nanocurcumin's Protective Role in Aluminum Phosphide-Induced Oxidative and Apoptotic Damage in rats

Shimaa S. El-Din<sup>1\*</sup>; Sherif M. Zaki<sup>2</sup>; Gaber H. Abdel-Fatah<sup>3</sup>; Engy Medhat<sup>1</sup> and Waleed A. Abd Algaleel<sup>4</sup>

<sup>1</sup>Department of Medical Biochemistry and Molecular biology, Faculty of Medicine, Cairo University, Egypt.

<sup>2</sup>Department of Physiological Sciences, MBBS program, Fakeeh College for Medical Sciences, Jeddah, Saudi Arabia.

<sup>3</sup>Department of Anatomy and Embryology, Faculty of Medicine, Beni-Suef University, Egypt.

<sup>4</sup>Department of Anatomy and Embryology, Faculty of Medicine, Cairo University, Egypt.

E-mail: [dr.shimaa.saad@cu.edu.eg](mailto:dr.shimaa.saad@cu.edu.eg)

### ARTICLE INFO

#### Article History

Received: 29/6/2025

Accepted: 3/8/2025

Available: 7/8/2025

#### Keywords:

Aluminum phosphide, nanocurcumin, lung injury, oxidative stress, apoptosis.

### ABSTRACT

Aluminum phosphide (AIP) is a very dangerous pesticide that gives off phosphine gas (PH<sub>3</sub>), which causes oxidative stress, lipid peroxidation, and mitochondrial dysfunction, especially in lung tissue. This results in inflammation, apoptosis, and severe pulmonary damage. Due to the absence of an effective antidote, alternative therapeutic strategies are urgently needed. This research investigates how nanocurcumin (NCU) can protect against lung damage caused by AIP by changing the oxidative stress and apoptosis pathways. Thirty-two rats were divided into four groups: Control, NCU-only, AIP, and AIP +NCU. We analyzed the lung tissue histologically and immunohistochemically. We evaluated the relative gene expression of Nrf2, SOD, CAT, PCNA, BAX, and BCL2 via real-time PCR. Quantitative image analysis was applied for histopathological scoring.

Results illustrated that exposure to AIP caused noticeable changes in tissue structure, such as inflammation, thickened walls between air sacs, and swelling of blood vessels. AIP-treated lungs significantly upregulated Caspase-3 and PCNA. AIP lowered the levels of SOD and CAT proteins and raised the BAX/BCL2 ratio, showing that it caused oxidative stress and enhanced apoptosis. NCU administration significantly reversed these effects, improving lung histology, reducing apoptosis markers, restoring antioxidant enzyme expression, and lowering the BAX/BCL2 ratio by 85% compared to the AIP group. Given its potent antioxidant and anti-apoptotic effects, NCU may represent a promising adjunct in future clinical detoxification protocols for aluminum phosphide poisoning. However, advancing this to clinical practice requires further investigation about dose optimization and pharmacokinetic studies to ensure safety and efficacy.

### INTRODUCTION

Aluminum phosphide (AIP) is an industrially used pesticide that poses a high toxicity risk, especially to non-target organisms, such as humans. These characteristics combined with its low cost, easy application process, and ability to preserve grains have made it one of the most effective grain preservation methods in use today, especially in resource-limited developing countries (Abdolghaffari *et al.*, 2015).

AIP is commonly known to be fatal on skin contact, inhalation, or ingestion. Multi-organ failure is the main cause of death in 30–70% of cases (Jafari *et al.*, 2015).

Aluminum phosphide toxicity exerts its harmful effect on lungs through the release of phosphine gas (PH<sub>3</sub>) and lipid peroxidation. This creates oxidative stress, causing harm to mitochondria and cellular structures (Hsu *et al.*, 1998). Oxidative stress has a pivotal role in AIP poisoning. Extensive research demonstrates that AIP exposure alters the oxidant-antioxidant equilibrium, leading to inflammatory responses, alveolar damage, and compromised breathing capacity (Kariman *et al.*, 2012). The lack of an effective antidote has restricted treatment strategies for these patients to only emergency symptom management. This shows the need for alternative therapeutic strategies to protect against AIP-mediated lung injury.

The polyphenolic compound curcumin, extracted from the rhizome root of the herb *Curcuma longa*, has been investigated for its wide range of antioxidant, anti-inflammatory, and cytoprotective activities (Menon and Sudheer, 2007). However, the clinical application of curcumin is limited due to its low bioavailability, rapid metabolism, and poor water solubility (Hussain *et al.*, 2017).

With recent advancements in nanotechnology, nanocurcumin (NCU) has been developed. This curcumin form has enhanced absorption, a longer half-life in the body, and higher tissue delivery than normal curcumin (Karthikeyan *et al.*, 2020). In vitro studies show that NCU has much stronger anti-inflammatory and antioxidant properties. This makes NCU a potentially useful molecule for treating lung damage caused by oxidative stress (Dende *et al.*, 2017).

Although NCU has several advantages, there is limited literature investigating its effects on AIP-induced lung damage. The aim of this study is to fill in this gap by looking into whether NCU can reduce the damage produced by AIP in the lungs by modulating the levels of oxidative stress.

Specifically, we examined the histopathological, immunohistochemical, and molecular changes in lung tissue. By elucidating the NCU's cytoprotective mechanisms, this research could pave the way for targeted therapies against AIP poisoning and other oxidative stress-related disorders.

## MATERIALS AND METHODS

### 1-Synthesis of Curcumin Nanoparticles:

Chitosan (MW 71.3 kDa, degree of deacetylation (89%)) was purchased from Aldrich (Germany), while sodium alginate (77%) was purchased from Sigma Chemical Co. (St. Louis, USA). Hexane, ethanol and dimethyl sulfoxide were purchased from Sigma Chemicals, India. All other reagents were purchased from Aldrich (Germany). Curcumin (95% total curcuminoid content) powder was obtained from the fisher scientific company.

Curcumin nanoparticles were prepared in accordance with (Basniwal *et al.*, 2014, and Abdel Wahab & Swaefy, 2020) protocols by extraction from curcumin powder, chitosan and sodium alginate (3:1 (v:v) at molar ratio) were used as carriers of curcumin nanoparticles.

Ten grams of curcumin powder were milled with hexane and 97% ethanol (1:1 (v: v) for 3 h. then 50 mg of curcumin was dissolved in dimethyl sulfoxide (15 ml) and left for 24 h at 3°C. Next 3 ml of curcumin solution was added into warm water (40°C), the mixture of chitosan and sodium alginate was added gradually and left for 6 h. under magnetic stirring at 30°C, after that the mixture was sonicated for 20 min with an ultrasonic power of 100 W and a frequency of 30 kHz. Subsequently, the mixture was centrifuged at 1500 rpm for 45 minutes, which was thereafter cooled in an ice bath and then the precipitate obtained was filtered, the end solution was then exposed to 1.5 psi of pressure for 10 hours discontinuously.

The morphology and size of the nanoparticles were examined by using a JEOL 1010 transmission electron microscope at 80 kV (JEOL, Japan). One drop of the nanoparticle solution was spread onto a

carbon-coated copper grid and was then dried at room temperature for transmission electron microscopy (TEM) analysis. The sizes were determined directly from the figure by using Image-Pro Plus 4.5 software. The value is an average size of three parallels.

## 2-Animals and Ethical Approval:

This study was conducted in compliance with ethical guidelines for animal research and was approved by the Institutional Animal Care and Use Committee (IACUC) under protocol number CU 0909203766 (9/09/2023). The experiment was done according to the National Research Council Guide for the Care and Use of Laboratory Animals and its related guidelines.

Thirty-two adults male Wistar rats (weighing 140–200 g) were obtained from the institutional animal house. Rats were housed in polypropylene cages under controlled environmental conditions: temperature ( $22 \pm 2^\circ\text{C}$ ), relative humidity (50–60%), and a 12-hour light/dark cycle. Standard chow and water were provided ad libitum. Animals were acclimatized to laboratory conditions for one week before the experiment.

## 3-Experimental Design and Grouping:

All rats were randomly distributed equally into four groups: Control group: received almond oil only (vehicle), NCU group: Administered nanocurcumin (8 mg/kg) orally for 5 days, AIP group: A single oral dose of AIP (12 mg/kg) dissolved in almond oil administered by gastric gavage, and AIP + NCU group: Administered both AIP (12 mg/kg) once and nanocurcumin (8 mg/kg) for 5 days.

To minimize bias, investigators were blinded to group assignments during histopathological, immunohistochemical, and PCR analyses. Rats were randomly assigned to treatment groups using a computerized random number generator.

## 4-Rationale for Sample Size and Dosage:

The sample size of eight animals per group was selected based on precedent from similar toxicological and gene expression studies involving aluminum phosphide-induced oxidative stress (Anand *et al.*, 2012; Kalpana and Menon 2004).

This sample size strikes a balance between ethical use of animals and sufficient sensitivity to detect differences in mortality, histopathology, and qPCR-based gene expression, consistent with accepted norms in rodent experimental toxicology.

Previous research determined the dose of AIP (12 mg/kg) based on its toxic mortality range (Haghi-Aminjan *et al.*, 2018). Also, oxidative stress was reduced in experimental models with NCU set at 8 mg/kg (Ghasemi *et al.*, 2023).

## 5-Humane Endpoints Monitoring:

We monitored each animal daily for possible signs of toxicity, variations in weight, food intake, and other activities. We developed humane endpoints to alleviate suffering, including weight loss (>20% of body weight), severe respiratory distress, and unresponsiveness to stimuli. At the end of day 5, rats were treated with an overdose of sodium pentobarbital (100 mg/kg i.p.) for euthanizing them.

## 6-Histological Sectioning:

Collected lung tissues were placed in 10% neutral-buffered formalin for 24 hours. The samples were dehydrated in graded alcohols, cleared in xylene, and paraffin embedded. The blocks were then sectioned at 5  $\mu\text{m}$  and stained for structure with H&E (Sheehan and Hrapchak, 1980).

## 7-Immunohistochemical Staining:

We conducted all immunohistochemistry using the guidelines prescribed by Ramos-Vara *et al.* (2008). Tissue blocks were heated at 95 degrees Celsius in citrate buffer (pH 6.0) for 10 minutes to remove the paraffin and rehydrate them. After turning off the body's own peroxidase, sections were covered in caspase-3 (1:200 dilution, Abcam, UK) and PCNA (1:150 dilution, Abcam, UK) primary antibodies and left to sit overnight at 4 degrees Celsius. A biotinylated secondary antibody was added to the cells, and then sections were looked at using a DAB chromogen system. Subsequently, the images were taken by a light microscope at a magnification of 40 $\times$  (Oktay *et al.*, 1995).

### 8-Real-Time PCR in Gene Expression Analysis:

Total RNA was extracted from rat lung tissues using the Qiagen RNeasy kit (Hilden, Germany). The spectrometer's NanoDrop measured the RNA purity (260/280 ratio). cDNA synthesis was carried out on the RevertAid First Strand cDNA Synthesis Kit (Thermo Fisher, USA). We used

the real-time SYBR Green PCR master mix method (Applied Biosystems, USA) to detect the relative gene expression of Nrf2, SOD, CAT, PCNA, BAX, and BCL2. Relative expression was evaluated using the  $2^{-\Delta\Delta CT}$  method. A housekeeping gene (GAPDH) was utilized to standardize results (Livak and Schmittgen, 2001). Table 1 shows the primer sequences.

**Table 1:** Primer sequences of the studied genes

Gene	Primer sequence
BAX	F: 5' CGGCGAATTGGAGATGAACTGG 3' R: 5' CTAGCAAAGTAGAAGAGGGCAACC 3'
BCL2	F: 5' TGTGGATGACTGACTACCTGAACC 3' R: 5' CAGCCAGGAGAAATCAAACAGAGG 3'
Nrf2	F: 5' CTCTCTGGAGACGGCCATGACT 3' R: 5' CTGGGCTGGGGACAGTGGTAGT 3'
SOD	F: 5' ACTGGTGGTCCATGAAAAGC 3' R: 5' AACGACTTCCAGCGTTTCCT 3'
CAT	F: 5' CGACCGAGGGATTCCAGATG 3' R: 5' ATCCGGGTCTTCTGTGCAA 3'
GAPDH	F: 5' GGTGGTCTCCTCTGACTTCAACA 3' R: 5' GTTGCTGTAGCCAAATTCGTTGT 3'

PCNA, proliferating cell nuclear antigen; Nrf2; NF-E2-related factor 2; SOD, superoxide dismutase; CAT, catalase; GAPDH, glyceraldehyde-3-phosphate dehydrogenase.

### 9-Statistical Analysis:

Data were analyzed using SPSS version 21.0 (IBM, USA). Results were expressed as mean  $\pm$  standard deviation (SD). We performed one-way analysis of variance (ANOVA) and Bonferroni post-hoc tests for multiple comparisons. A p-value  $< 0.05$  was considered statistically significant.

## RESULTS

### 1.1-Nanoparticle Characterization:

Nanoparticles were uncontrolled in shape with a size range of nearly (32-39 nm) with crystal structure suspension and 98.5% purity (Fig. 1).

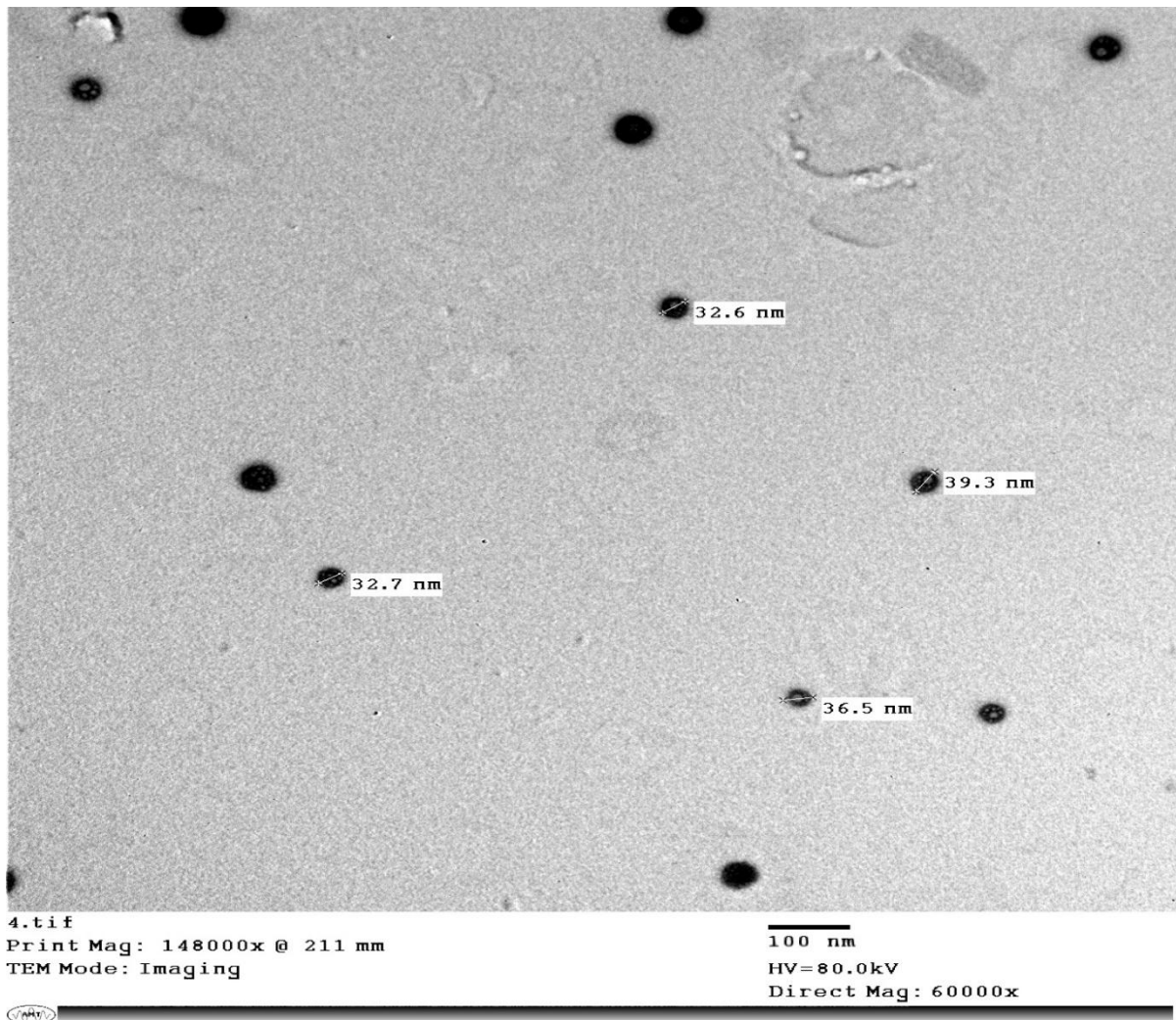


**Fig. 1:** TEM picture of curcumin nanoparticles.

### 1.2-Lung Structure Revealed by H&E Staining:

The histological scoring of lung damage was assessed. Inflammation, alveolar thickening, and vascular congestion were the essential markers of pulmonary injury. In the control group, all parameters exhibited a standard score of 1.0, indicating no significant histological alterations (Figs. 2, 3-a). In the same way, the NCU group's lung tissue structure didn't change much; inflammation scored 1.1, while alveolar thickening and vascular congestion stayed at 1.0 (Fig. 2). This suggests that NCU

administration alone doesn't cause histological lung damage

The AIP group showed the highest severity scores, with inflammation (4.5), alveolar thickening (3.8), and vascular congestion (4.2). These findings indicate that AIP induces significant pulmonary injury (Figs 2, 3 b-c). The AIP + NCU group exhibited a considerable reduction in lung damage severity compared to the AIP group. Inflammation scores decreased to 2.2, alveolar thickening decreased to 1.9, and vascular congestion decreased to 2.0. These reductions imply that NCU administration reduces AIP-induced lung injury (Figs 2, 3-d).

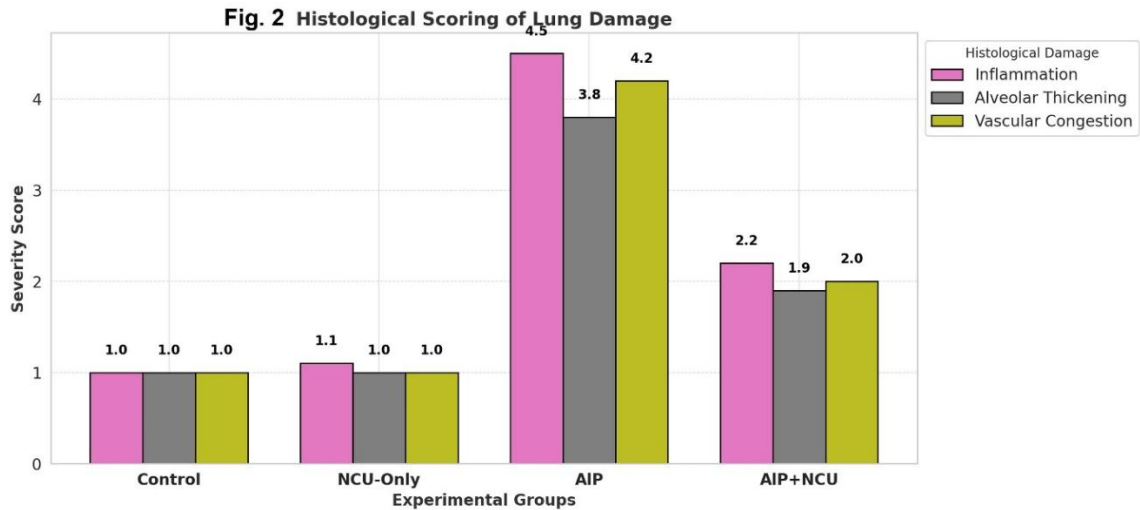


**Fig. 2:** Bar chart shows how the lung damage was scored by histology in the experimental groups. Three histological parameters were assessed: inflammation, alveolar thickening and vascular congestion.

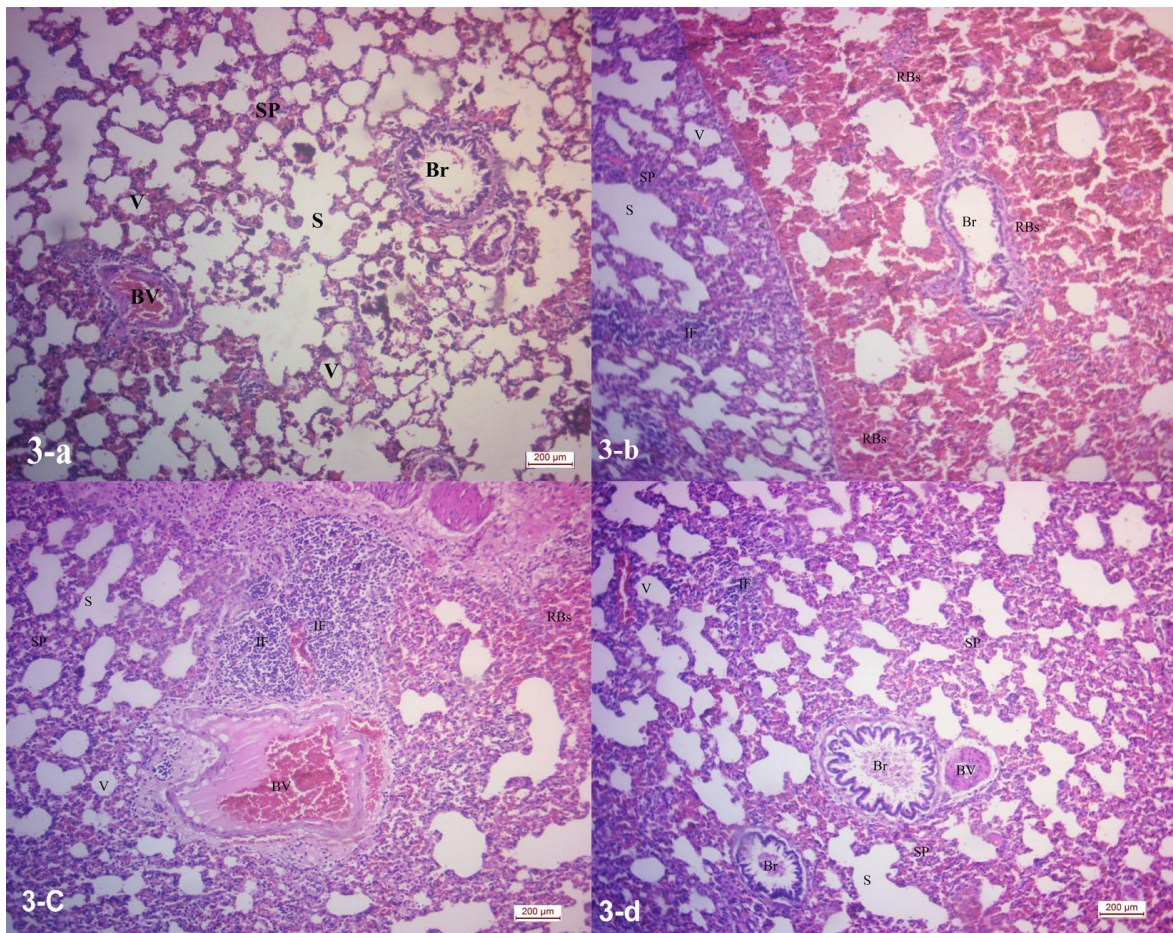


**Fig. 3:** The morphology of the lungs in various groups. Alveolar sacs (S), alveoli (V), interalveolar septa (SP), bronchi (Br), and blood vessels (BV). **a:** shows the normal lung architecture of a control rat. **b & c:** show inflammatory cells (IF), the interalveolar septa getting thicker (SP), blood vessels getting bigger (BV), and blood leaking out (RB) after rats were given AIP. **d:** There were no problems with the lungs of the AIP+NCU rat, but the interalveolar septa (SP) were thicker, and there were cells that caused inflammation (IF). The scale bar measures 200 μm (a-d) in H & E.

### 1.3-The General Toxicological Data:

The mortality graph indicates that 50% of rats in the AIP-treated group died, while the co-administration of NCU significantly reduced mortality to 17% (Fig. 4-a). Other than these rats, the remaining rats in all the groups continued to consume food and water, exhibiting stable health conditions overall.

In the AIP group, mortality occurred within 24–48 hours following aluminum phosphide administration. The deaths were consistently preceded by observable toxicological signs, including hypoactivity, piloerection, breathlessness, and progressive weight loss. All gavage administrations were

performed by trained personnel under direct supervision. Necropsy examinations revealed no evidence of mechanical trauma, hemorrhage, or esophageal damage that would suggest a procedural cause of death. In contrast, the AIP + NCU co-treated group showed improved outcomes, with mortality reduced to 17%, indicating a protective effect of NCU.

The average weight among all rats was  $122.5 \pm 8.8$  g as the starting weight. The body weight loss graph reveals that AIP exposure caused a 23% weight reduction, whereas the AIP + NCU group exhibited a lesser 10% weight loss with significant difference between both groups (Fig. 4-b).

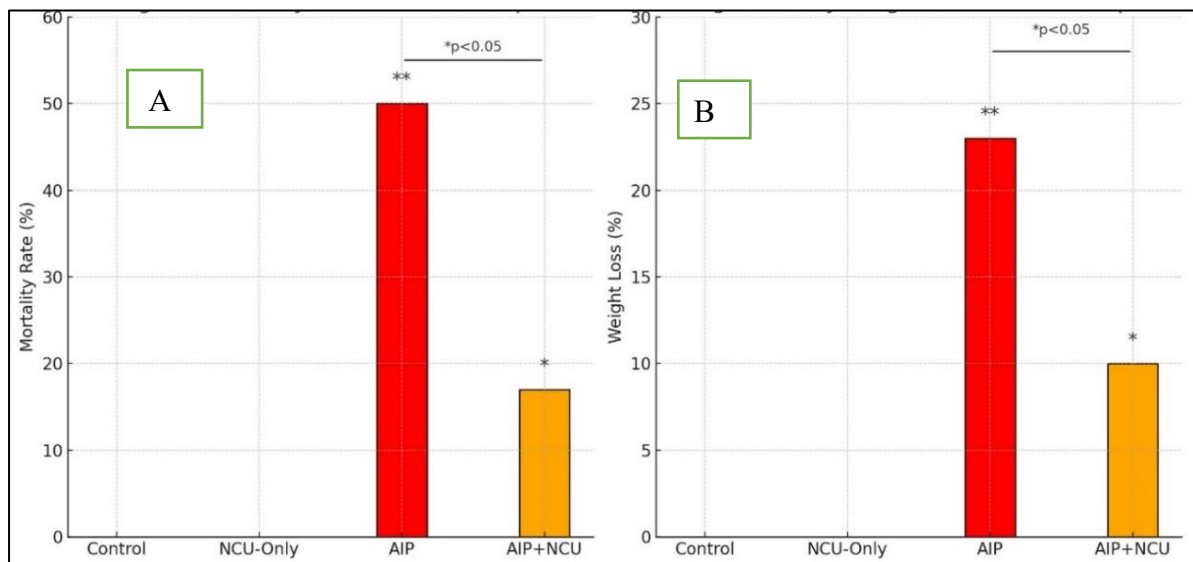


**Fig. 4-a:** Mortality rates among study groups. **4-b:** Percentage of body weight loss among study groups. \* significant difference at  $p < 0.05$ , \*\* highly significant difference at  $p < 0.001$ .

### 1.4-Immunohistochemical Assessment of Caspase-3 and PCNA:

The immunohistochemical evaluation revealed critical insights into the apoptotic and regenerative responses of lung tissue following aluminum phosphide (AIP) exposure and nanocurcumin (NCU) intervention.

#### **Caspase-3 Expression:**

In the AIP-treated group, there was a marked upregulation of caspase-3 immunoreactivity, with widespread brown cytoplasmic staining evident in alveolar and

bronchial epithelial cells. This elevation ( $30.0 \pm 7.9\%$ ;  $p < 0.001$ ) indicates heightened apoptotic activity triggered by AIP-induced oxidative stress and mitochondrial dysfunction (Figs. 5c & 7).

Co-treatment with NCU significantly attenuated this expression to  $12.6 \pm 2.8\%$ , with a visibly reduced staining intensity and distribution, suggesting a protective, anti-apoptotic effect of nanocurcumin (Figs. 5d & 7).

In both NCU-only and control groups, caspase-3 expression remained low and



comparable ( $5.2 \pm 2.1\%$  vs.  $4.0 \pm 1.6\%$ ), affirming the non-toxic profile of NCU under

basal physiological conditions (Figs. 5b,5a&7).

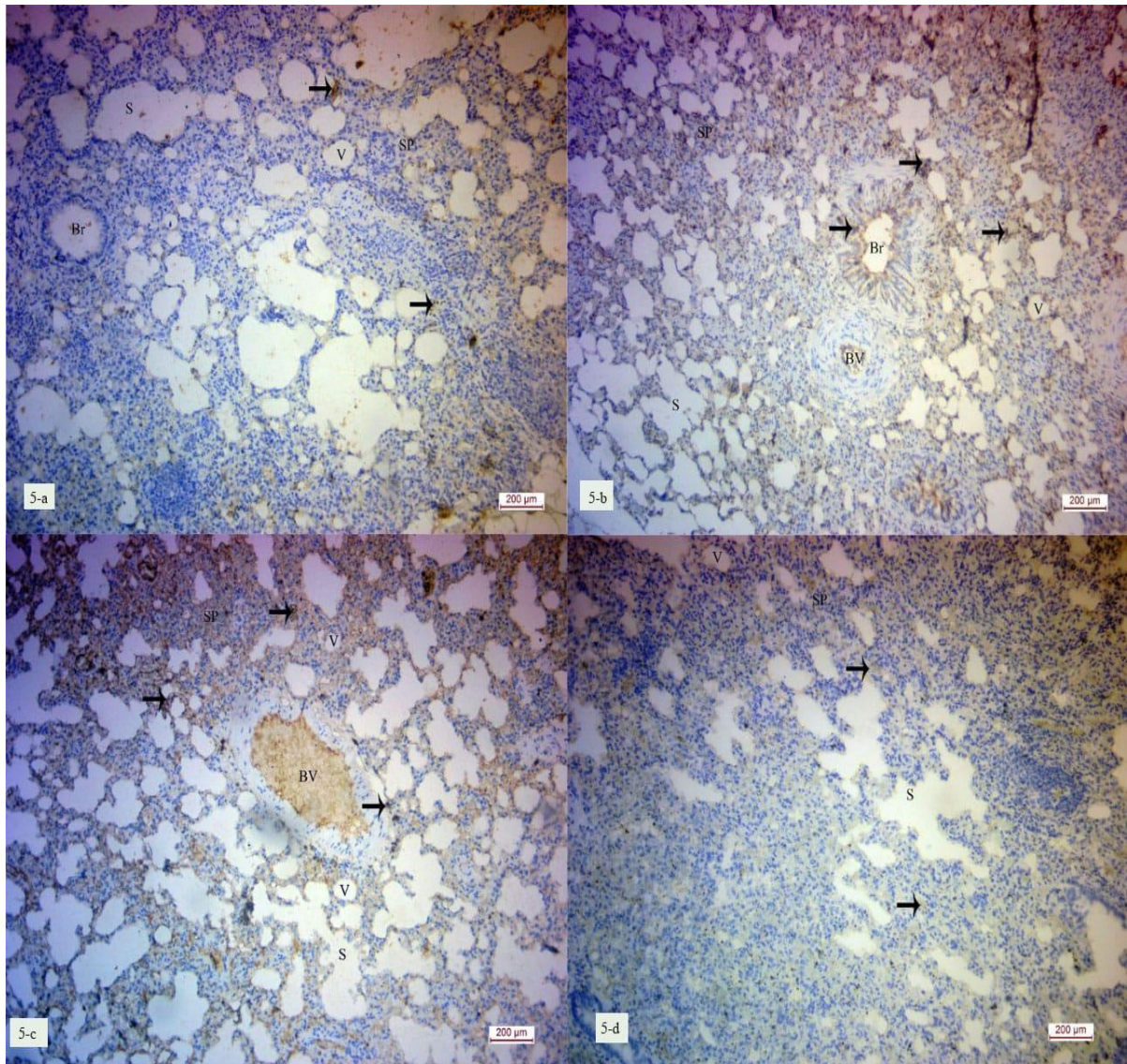


**Fig. 5:** Caspase-3 immunohistochemistry of lung tissue in different study groups (a) Control group, (b) NCU group, (c) AIP group, (d) AIP + NCU group.

#### ***PCNA Expression:***

PCNA staining, used to detect cellular proliferation or repair activity, was significantly increased in the AIP group ( $38.8 \pm 6.3\%$ ;  $p < 0.001$ ), with strong nuclear localization in alveolar and bronchial epithelium. This increase likely reflects compensatory hyperplasia in response to tissue injury (Fig. 6c).

The AIP + NCU group demonstrated a notable reduction in PCNA expression ( $23.2 \pm 3.3\%$ ), indicating reduced proliferative stress and histological improvement (Figs. 6.d&7).

The NCU-only group again paralleled the control ( $14.0 \pm 2.0\%$  vs.  $12.8 \pm 1.9\%$ ), supporting the safety and biological neutrality of nanocurcumin in normal lung tissue (Figs. 6b, 6a&7).

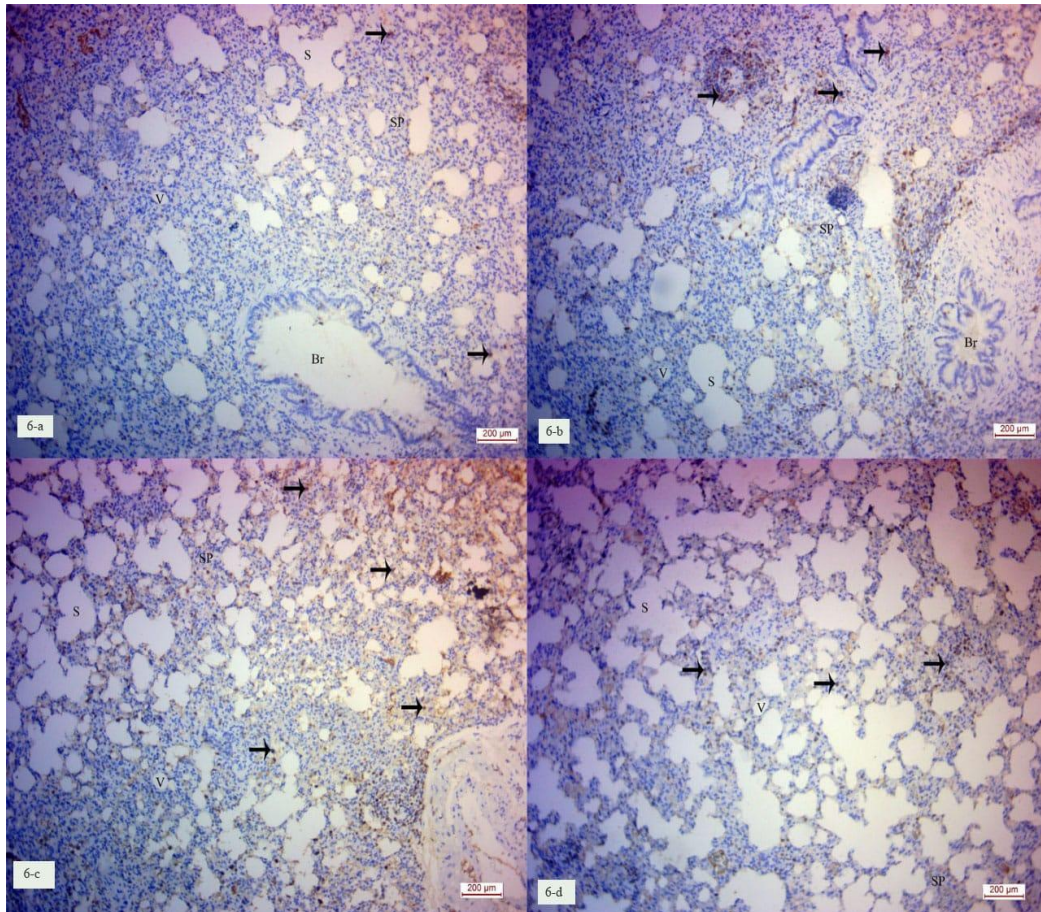


**Fig. 6:** PCNA immunohistochemistry of lung tissue in different study groups (a) Control group, (b) NCU group, (c) AIP group, (d) AIP + NCU group.

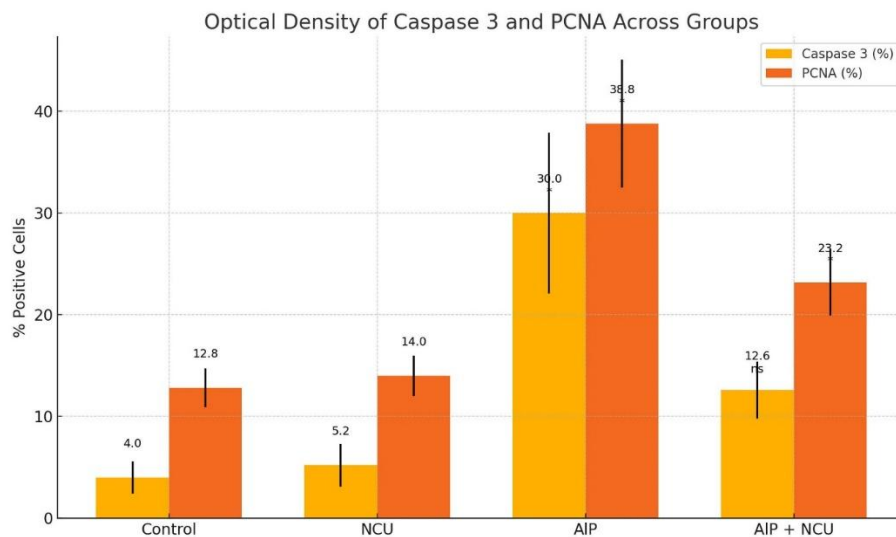


**Fig. 7:** Quantitative analysis of caspase-3 and PCNA positive cells among experimental groups. Bar chart shows the percentage of caspase-3 and PCNA immune-positive cells. Aluminum phosphide (AIP) exposure significantly increased both caspase-3 and PCNA expression compared to control ( $p < 0.001$ ), indicating elevated apoptotic and proliferative activity. Co-treatment with Nanocurcumin (AIP + NCU) markedly reduced both markers relative to the AIP group ( $p < 0.001$ ), demonstrating a protective effect. The NCU group alone showed no significant difference from the control, suggesting that Nanocurcumin does not induce apoptosis or proliferation under basal conditions. Values are expressed as mean  $\pm$  SD.

## 1.5-Relative Gene Expression Analysis via Real-Time PCR:

### 1.5.1-Oxidative Stress Markers:

Exposure to AIP led to a marked downregulation in the relative gene expression of Nrf2, SOD, and CAT, indicating significant oxidative stress and impaired antioxidant defense. AIP-treated samples exhibited significant reduction to 0.21 for Nrf2, 0.31 for SOD, and 0.19 for

CAT, compared to control values approximating unity (1.02–1.03). In contrast, when NCU was added to the treatment (AIP + NCU group), it greatly improved the situation, bringing the levels of Nrf2, SOD, and CAT back up to 0.83, 0.78, and 0.76, respectively. The NCU-only group showed similar levels of the three genes as the control group, indicating that NCU alone does not change antioxidant gene expression (Fig. 8).

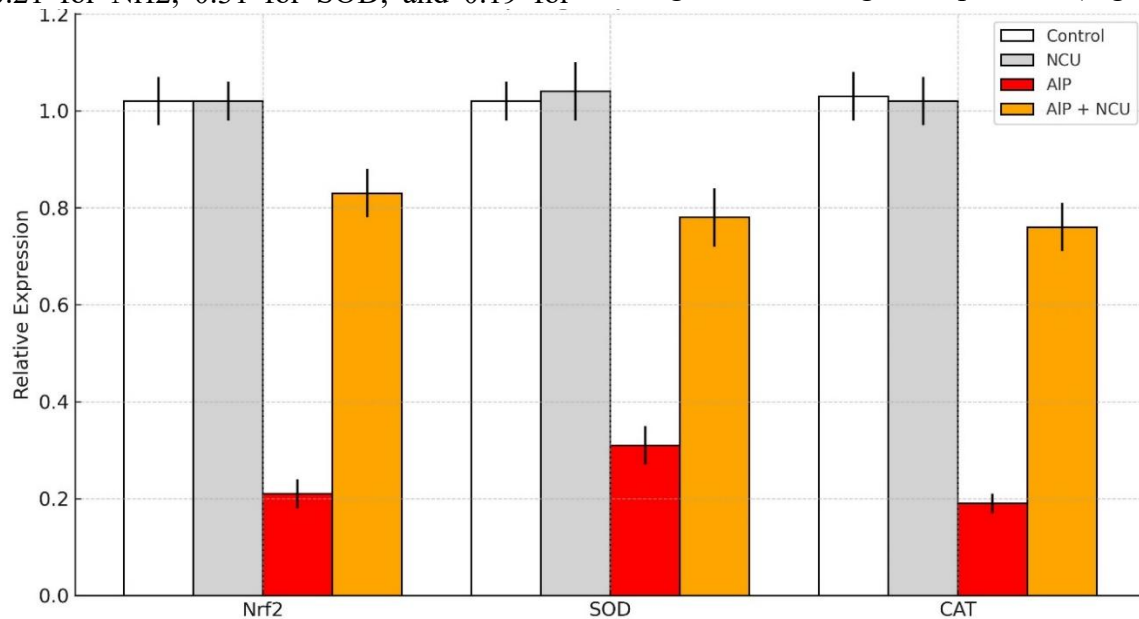


**Fig. 8:** Relative mRNA expression levels of antioxidant genes (Nrf2, SOD, and CAT) across experimental groups. Gene expression was significantly downregulated in the AIP group compared to the control, indicating oxidative stress and impaired antioxidant response. Co-treatment with Nanocurcumin (AIP + NCU) markedly restored expression levels of Nrf2, SOD, and CAT ( $p < 0.05$ ). The NCU-only group exhibited expression profiles approaching the control group.

### 1.5.2-Apoptotic Markers:

In the AIP-treated group, there was a significant upregulation of BAX (4.28-fold) coupled with a profound downregulation of BCL2 (0.15-fold), resulting in an elevation of the BAX/BCL2 ratio (20.12), indicative of a strong pro-apoptotic shift. Conversely, co-treatment with Nanocurcumin (AIP + NCU group) significantly attenuated BAX expression (2.24) and restored BCL2 levels

(0.80), thereby reducing the BAX/BCL2 ratio to 2.83. The NCU-only group showed expression levels of BAX (0.98), BCL2 (1.01), and BAX/BCL2 ratio (1.00) comparable to the control group, indicating that Nanocurcumin alone does not disrupt apoptotic balance. These findings confirm the potent apoptotic effect of AIP and emphasize the protective role of Nanocurcumin in reducing apoptosis signalling pathways (Fig. 9).

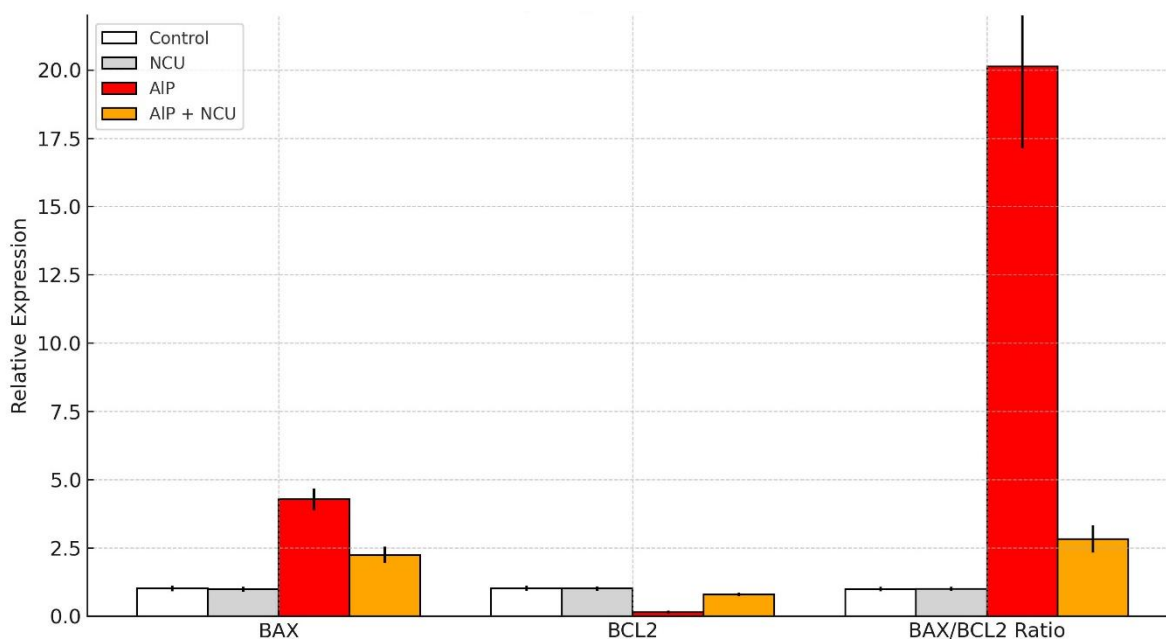


**Fig. 9:** Relative mRNA expression of apoptosis-related genes (BAX, BCL2) and BAX/BCL2 ratio across experimental groups. Aluminum phosphide (AIP) exposure resulted in significant upregulation of the pro-apoptotic gene BAX and downregulation of the anti-apoptotic gene BCL2, leading to a marked increase in the BAX/BCL2 ratio (20.12), indicating enhanced apoptotic activity. Co-treatment with Nanocurcumin (AIP + NCU) significantly diminished these changes by reducing BAX expression and partially restoring BCL2 levels, thus lowering the BAX/BCL2 ratio to 2.83. The NCU-only group showed gene expression profiles comparable to the control group.

## DISCUSSION

In this study, giving AIP at a dose of 12 mg/kg caused a 50% death rate, which matches its known lethal dose range of 8.7–12.5 mg/kg (Jafari *et al.*, 2015). Co-administration of nanocurcumin (NCU) significantly reduced mortality to 17%, highlighting its protective effect against AIP-induced toxicity. Additionally, AIP exposure led to a substantial reduction in body weight, whereas rats co-treated with NCU exhibited only a 10% weight loss, suggesting attenuation of systemic toxicity. These clinical features align with previously reported manifestations of AIP-induced systemic toxicity due to phosphine gas release and mitochondrial dysfunction, rather than procedural complications such as gavage-related aspiration (Haghi-Aminjan *et al.*, 2018; Sciuto *et al.*, 2016).

Histologically, AIP exposure produced pronounced lung damage characterized by alveolar thickening,

interstitial inflammation, vascular congestion, and hemorrhage. These findings are consistent with the known pulmonary toxicity of AIP, which is closely linked to oxidative injury (Sciuto *et al.*, 2016). In contrast, the NCU-treated group exhibited preserved lung architecture, reduced inflammatory infiltration, and improved vascular integrity, as reflected in the significantly lower histopathological damage scores.

The mechanistic underpinning of this injury is primarily attributed to oxidative stress, which arises from an imbalance between reactive oxygen species (ROS) production and the antioxidant defense system (Birben *et al.*, 2012; Mccord, 1993). AIP exposure greatly reduced the levels of important antioxidant enzymes: SOD by approximately 70%, and CAT by 81%, relative to the control group. This corresponds to a reduction in CAT expression to 0.19-fold compared to baseline levels. This decline is in line with previous studies documenting AIP-

induced oxidative depletion (Kariman *et al.*, 2012; Shakeri and Mehrpour, 2014). SOD catalyzes the conversion of superoxide radicals into hydrogen peroxide, which is subsequently detoxified by CAT. Thus, their suppression contributes to the accumulation of ROS and ensuing tissue damage (Wang *et al.*, 2018).

NCU administration restored SOD and CAT gene expression where a significant difference is shown compared to the AIP group, supporting its role in redox balance. These antioxidant effects are attributed to the phenolic structure of curcumin, which enables ROS scavenging, enzyme modulation, and inhibition of free radical-generating enzymes (Marchiani *et al.*, 2014; Rathore *et al.*, 2020).

The protective effects of NCU are further supported by its ability to enhance Nrf2 expression (Rajabi *et al.*, 2024). Nrf2 is a master regulator of the antioxidant response. The observed upregulation of Nrf2 in the AIP + NCU group suggests activation of the Nrf2–ARE (antioxidant response element) pathway, which is known to induce the transcription of various cytoprotective genes, including heme oxygenase-1 (HO-1) and NAD(P)H quinone dehydrogenase 1 (NQO1) (Menon and Sudheer, 2007; Panahi *et al.*, 2016; Saad El-Din *et al.*, 2020). Even though this study didn't directly measure these downstream effectors, their known functions in reducing oxidative stress and protecting mitochondria highlight how nanocurcumin might work to protect cells. Future studies are needed to check the activity of these downstream genes and confirm that the Nrf2–ARE signalling pathway is fully activated. The upregulation of Nrf2 in the NCU treated group thus confirms its involvement in cellular defense mechanisms, including antioxidant, anti-inflammatory, and anti-apoptotic pathways.

At the molecular level, AIP significantly increased caspase-3 expression, indicating activation of the intrinsic apoptotic pathway (Pu *et al.*, 2017; Li *et al.*, 2015). This was further supported by a two-fold rise in PCNA, suggesting increased cellular turnover

or repair in response to injury. The apoptosis pathway was additionally confirmed by changes in BAX and BCL-2 expression. AIP-treated lungs showed upregulation of pro-apoptotic BAX and marked downregulation of anti-apoptotic BCL-2, resulting in a 20-fold elevation in the BAX/BCL-2 ratio—an established indicator of apoptotic sensitivity (Abdel Fattah *et al.*, 2023). These alterations were mitigated by NCU co-treatment, which reduced caspase-3 and BAX expression, restored BCL-2 levels, and decreased the BAX/BCL-2 ratio to near-control values. Our findings could provide a foundation for future clinical applications aimed at improving outcomes in cases of AIP poisoning.

### Conclusion

This study demonstrates that curcumin nanoparticles (NCU) significantly attenuate the histopathological and molecular alterations induced by aluminum phosphide in lung tissue. The protective effect of NCU is primarily mediated through the modulation of oxidative stress, as evidenced by the restoration of SOD, CAT, and Nrf2 expression, along with the suppression of caspase-3, PCNA, and the BAX/BCL-2 ratio. Given its potent antioxidant and anti-apoptotic effects, NCU may represent a promising adjunct in future clinical detoxification protocols for aluminum phosphide poisoning. However, clinical translation will require dose-optimization studies, pharmacokinetic profiling, and validation in human trials to ensure safety and efficacy.

### List of Abbreviations

Name	Abbreviation
Aluminum phosphide	(AIP)
phosphine gas	(PH <sub>3</sub> )
nanocurcumin	(NCU)

### Declarations:

**Ethical Approval:** This study was conducted in compliance with ethical guidelines for animal research and was approved by the Institutional Animal Care and Use Committee (IACUC) under protocol number CU 0909203766 (9/09/2023).

**Competing interests:** The authors declare no conflicts of interest.

**Contributions:** All authors contributed equally, and have read and agreed to the published version of the manuscript.

**Funding:** This research was self-funded and received no funding from any sources.

**Availability of Data and Materials:** The data presented in this study are available on request from the corresponding author.

**Acknowledgements:** The authors acknowledge the kind help of Dr. Mohamed M. Abdel Wahab, Professor of Plant Physiology, Faculty of Agriculture, Cairo University, Egypt.

#### REFERENCES

- Abdel Fattah S, Ibrahim MEE, El-Din SS, Emam HS, Algaleel WAA. (2023). Possible therapeutic role of zinc oxide nanoparticles versus vanillic acid in testosterone-induced benign prostatic hyperplasia in adult albino rat: A histological, immunohistochemical and biochemical study. *Life Sciences*, Dec 1;334:122190.
- Abdel Wahab MM and Swaefy HM. (2020). Comparison between Commercial and Nano NPK in Presence of Nano Zeolite on Sage Plant Yield and its Components under Water Stress. *Agriculture (Pol'nohospodárstvo)*, 66, (1): 24 – 39. DOI: 10.2478/agri-2020-0003
- Abdolghaffari AH, Baghaei A, Solgi R, Gooshe M, Baeri M, Navaei-Nigjeh M, et al. (2015). Molecular and biochemical evidences on the protective effects of triiodothyronine against phosphine-induced cardiac and mitochondrial toxicity. *Life Sciences*, 139:30-9.
- Anand R, Kumari P, Kaushal A, Bal A, Wani WY, Sunkaria A, et al. (2012). Effect of acute aluminum phosphide exposure on rats: a biochemical and histological correlation. *Toxicology Letters*, 215(1): 62-69.
- Basniwal, RK, Khosla R, & Jain N. (2014). Improving the anticancer activity of curcumin using nanocurcumin dispersion in water. *Nutrition and cancer*, 66(6), 1015–1022. <https://doi.org/10.1080/01635581.2014.936948>
- Birben E, Sahiner UM, Sackesen C, Erzurum S, Kalayci O. (2012). Oxidative stress and antioxidant defense. *World allergy organization journal*, 5:9-19.
- Dende C, Meena J, Nagarajan P, Nagaraj VA, Panda AK, Padmanaban G. (2017). Nanocurcumin is superior to native curcumin in preventing degenerative changes in Experimental Cerebral Malaria. *Scientific reports*, 7(1):10062.
- Ghasemi SZ, Beigoli S, Behrouz S, Gholamnezhad Z, Mohammadian Roshan N, Boskabady MH. (2023). Evaluation of nano-curcumin against inhaled paraquat-induced lung injury in rats. *Pharmacological reports*, 75(3), 671–681.
- Haghi-Aminjan H, Baeri M, Rahimifard M, Alizadeh A, Hodjat M, Hassani S, et al. (2018). The role of minocycline in alleviating aluminum phosphide-induced cardiac hemodynamic and renal toxicity. *Environmental toxicology and pharmacology*, 64:26-40.
- Hsu C-H, Quistad GB, Casida JE. (1998). Phosphine-induced oxidative stress in Hepa 1c1c7 cells. *Toxicological sciences*, 46(1):204-10.
- Hussain Z, Thu HE, Amjad MW, Hussain F, Ahmed TA, Khan S. (2017). Exploring recent developments to improve antioxidant, anti-inflammatory and antimicrobial efficacy of curcumin: A review of new trends and future perspectives. *Materials science and engineering: C*, 77:1316-26.
- Jafari A, Baghaei A, Solgi R, Baeri M, Chamanara M, Hassani S, et al. (2015). An electrocardiographic, molecular and biochemical approach to explore the cardioprotective effect of vasopressin and milrinone against

- phosphide toxicity in rats. *Food and chemical toxicology*, 80:182-92.
- Kalpana C, Menon VP. (2004). Modulatory effects of curcumin on lipid peroxidation and antioxidant status during nicotine-induced toxicity. *Polish journal of pharmacology*, 56(5), 581–586.
- Kariman H, Heydari K, Fakhri M, Shahrami A, Dolatabadi AA, Mohammadi HA, et al. (2012). Aluminium phosphide poisoning and oxidative stress: serum biomarker assessment. *Journal of Medical Toxicology*, 8:281-4.
- Karthikeyan A, Senthil N, Min T. (2020). Nanocurcumin: A promising candidate for therapeutic applications. *Frontiers in Pharmacology*, 11:529594.
- Li J, Meng Z, Zhang G, Xing Y, Feng L, Fan S, et al. (2015). N-acetylcysteine relieves oxidative stress and protects hippocampus of rat from radiation-induced apoptosis by inhibiting caspase-3. *Biomed Pharmacother*, 70:1-6.
- Livak KJ, Schmittgen TD. (2001). Analysis of relative gene expression data using real-time quantitative PCR and the 2(-Delta Delta C(T)) Method. *Methods*, 25(4):402-8.
- Marchiani A, Rozzo C, Fadda A, Delogu G, Ruzza P. (2014). Curcumin and curcumin-like molecules: from spice to drugs. *Current medicinal chemistry*, 21(2):204-22.
- Mccord JM. (1993). Human disease, free radicals, and the oxidant/antioxidant balance. *Clinical Biochemistry*, 26(5):351-7.
- Menon VP, Sudheer AR. (2007). Antioxidant and anti-inflammatory properties of curcumin. *Advances in experimental medicine and biology*, 595, 105–125.
- Menon VP, Sudheer AR. (2007). Antioxidant and anti-inflammatory properties of curcumin. The molecular targets and therapeutic uses of curcumin. *Health and Disease*, 595:105-125.
- Oktaý K, Schenken RS, Nelson JF. (1995). Proliferating cell nuclear antigen marks the initiation of follicular growth in the rat. *Biology of Reproduction*, 53(2), 295–301.
- Panahi Y, Alishiri GH, Parvin S, Sahebkar A. (2016). Mitigation of systemic oxidative stress by curcuminoids in osteoarthritis: results of a randomized controlled trial. *Journal Of Dietary Supplements*, 13(2):209-220.
- Pu X, Storr SJ, Zhang Y, Rakha EA, Green AR, Ellis IO, et al. (2017). Caspase-3 and caspase-8 expression in breast cancer: caspase-3 is associated with survival. *Apoptosis*, 22:357-368.
- Rajabi S, Darroudi M, Naseri K, Farkhondeh T, Samarghandian S. (2024). Protective Effects of Curcumin and its Analogues via the Nrf2 Pathway in Metabolic Syndrome. *Current medicinal chemistry*, 31(25), 3966–3976.
- Ramos-Vara JA, Kiupel M, Baszler T, Bliven L, Brodersen B, Chelack B, et al. (2008). Suggested guidelines for immunohistochemical techniques in veterinary diagnostic laboratories. *Journal of veterinary diagnostic investigation: official publication of the American Association of Veterinary Laboratory Diagnosticians, Inc*, 20(4), 393–413. <https://doi.org/10.1177/104063870802000401>.
- Rathore S, Mukim M, Sharma P, Devi S, Nagar JC, Khalid M. (2020). Curcumin: A review for health benefits. *International Journal of Research and Review*, 7(1):273-90.
- Saad El-Din S, Rashed L, Medhat E, Emad Aboulhoda B, Desoky Badawy A, Mohammed ShamsEldeen A, Abdelgwad M. (2020). Active form of vitamin D analogue mitigates neurodegenerative changes in

- Alzheimer's disease in rats by targeting Keap1/Nrf2 and MAPK-38p/ERK signaling pathways. *Steroids*, April, 156:108586. doi: 10.1016/j.steroids.2020.108586.
- Sciuto AM, Wong BJ, Martens ME, Hoard-Fruchey H, Perkins MW. (2016). Phosphine toxicity: a story of disrupted mitochondrial metabolism. *Annals of the New York Academy of Sciences*, 1374(1), 41–51.
- Shakeri S, Mehrpour O. (2014). Aluminum phosphide poisoning in animals. *International Journal of Medical Toxicology and Forensic Medicine*, 5(2):81-97.
- Sheehan DC, Hrapchak BB. (1980). Theory and practice of histotechnology. 2d ed. St. Louis: Mosby; xiii, 481 p. p.
- Wang Y, Branicky R, Alycia Noë A, Hekimi S. (2018). Superoxide dismutases: Dual roles in controlling ROS damage and regulating ROS signaling. *The Journal of cell biology*, 217(6), 1915–1928.